ACS APPLIED MATERIALS & INTERFACES

Letter

www.acsami.org

Doped Lanthanum Nickelates with a Layered Perovskite Structure as Bifunctional Cathode Catalysts for Rechargeable Metal–Air Batteries

Kyu-Nam Jung,[†] Jong-Hyuk Jung,[†] Won Bin Im,[‡] Sukeun Yoon,[†] Kyung-Hee Shin,[†] and Jong-Won Lee*[,§]

[†]Energy Efficiency and Materials Research Division, Korea Institute of Energy Research, 152 Gajeong-ro, Yuseong-gu, Daejeon, 305-343, Republic of Korea

[‡]School of Materials Science and Engineering, Chonnam National University, 77 Yongbong-ro, Buk-gu, Gwangju 500-757, Republic of Korea

[§]New and Renewable Energy Research Division, Korea Institute of Energy Research, 152 Gajeong-ro, Yuseong-gu, Daejeon, 305-343, Republic of Korea

Supporting Information

ABSTRACT: Rechargeable metal–air batteries have attracted a great interest in recent years because of their high energy density. The critical challenges facing these technologies include the sluggish kinetics of the oxygen reduction–evolution reactions on a cathode (air electrode). Here, we report doped lanthanum nickelates (La_2NiO_4) with a layered perovskite structure that serve as efficient bifunctional electrocatalysts for oxygen reduction and evolution in an aqueous alkaline electrolyte. Rechargeable lithium–air and zinc–air batteries assembled with these catalysts exhibit remarkably reduced discharge–charge voltage gaps (improved round-trip efficiency) as well as high stability during cycling.

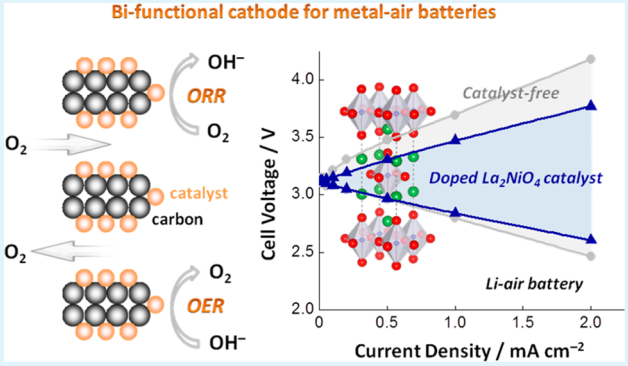

KEYWORDS: *metal–air battery, bifunctional catalyst, oxygen reduction, oxygen evolution, layered perovskite*

INTRODUCTION

Rechargeable metal–air batteries based on lithium–oxygen and zinc–oxygen chemistries have higher theoretical energy density than state-of-the-art lithium-ion batteries.[1−4] If successfully developed, they could enable electric vehicles with driving ranges similar to those of gasoline-powered vehicles. During discharge, a metal-air battery generates electricity through an oxidation reaction of a metal anode (Li or Zn), and a reduction reaction of oxygen (O_2) on a porous cathode. The reverse reactions occur upon charge. Metal-air batteries under development suffer from slow rates of the oxygen reduction reaction (ORR) and the oxygen evolution reaction (OER), which results in large discharge–charge overpotentials (i.e., large voltage gaps and low round-trip efficiency).[2−4] Thus, reducing the overpotentials for both ORR and OER via "bifunctional" electrocatalysts is of great importance for improving round-trip efficiency and cyclability.

The catalysts that have been typically utilized for ORR and OER are made up of precious metals, such as Pt and Ir.[5−7] Their high cost, however, limits widespread use in large-scale applications. Significant progress has been made over the years in the development of cost-effective catalysts based on mixed transition metal oxides.[8−17] Among various types of metal oxides, perovskites have recently received a lot of attention due to their high catalytic activity and stability in aqueous alkaline electrolytes.[12,14−17] Yang et al.[12] synthesized the $Sr_{0.95}Ce_{0.05}CoO_3$ (SCCO) perovskite catalysts loaded with Cu and demonstrated their bifunctionality in rechargeable Li–air batteries. They reported a considerable improvement in the round-trip efficiency of a battery with the SCCO-Cu catalyst compared to that of a catalyst-free battery. Several studies have also reported bifunctional ORR-OER activity for nanostructured $La_{0.6}Ca_{0.4}CoO_3$,[14] $LaNiO_3$,[15] and $La_{0.8}Sr_{0.2}MnO_3$ catalysts,[16] suggesting that these catalysts can enhance the round-trip efficiency of metal-air batteries. As mentioned above, the investigations into perovskite-type catalysts for metal-air batteries to date have mainly focused on "simple" perovskites with the general formula of AMO_3, where A is a rare earth metal and M is a transition metal. A recent experimental study[17] suggested that easily removable oxygen in the Ruddlesden–Popper-type $LaSr_3Fe_3O_{10}$ "layered" perovskite facilitates the redox reaction of the transition metal, thereby leading to enhanced ORR and OER activity.

In this work, we report doped lanthanum nickelates (La_2NiO_4) with a "layered" perovskite structure that are highly active for ORR and OER in metal-air batteries. Unlike a simple perovskite, an A_2MO_4 layered perovskite consists of AMO_3 (perovskite) and AO (rock salt) layers alternating in the *c* direction (Figure 1a).[18,19] Doping of aliovalent cations onto

Received: August 6, 2013
Accepted: September 20, 2013
Published: September 20, 2013

   dx.doi.org/10.1021/am403244k | ACS Appl. Mater. Interfaces 2013, 5, 9902–9907

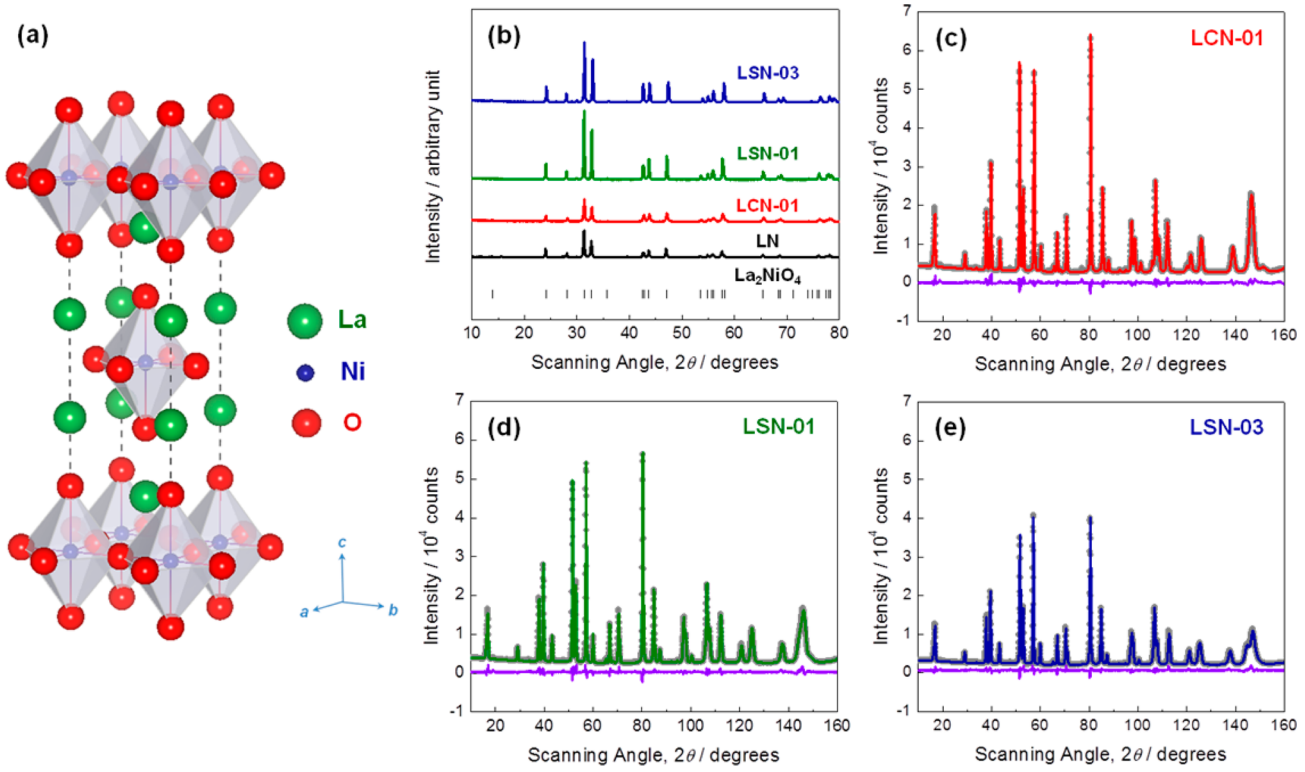

Figure 1. (a) Crystal structure of an La_2NiO_4 layered perovskite. (b) XRD patterns for La_2NiO_4 (LN), $La_{1.9}Ca_{0.1}NiO_4$ (LCN-01), $La_{1.9}Sr_{0.1}NiO_4$ (LSN-01), and $La_{1.7}Sr_{0.3}NiO_4$ (LSN-03) and (c–e) NPD patterns. The gray symbols in c– e are the observed patterns, and the solid lines represent the patterns calculated by the Rietveld method. A difference (obsd − calcd) plot is shown beneath.

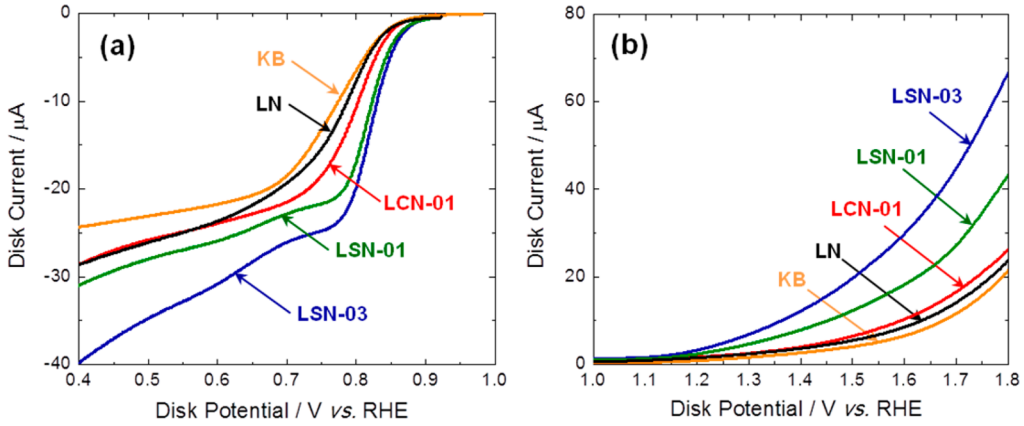

Figure 2. Polarization curves of catalyst-free Ketjen Black (KB), La_2NiO_4 (LN), $La_{1.9}Ca_{0.1}NiO_4$ (LCN-01), $La_{1.9}Sr_{0.1}NiO_4$ (LSN-01), and $La_{1.7}Sr_{0.3}NiO_4$ (LSN-03) measured for (a) ORR and (b) OER. The RDE measurements were performed in 0.1 M KOH with a scan rate of 10 mV s^{-1} and a rotation rate of 1200 rpm. Ohmic potential drop was not compensated for in the measurement.

A_2MO_4 controls lattice defects (M^{3+} and/or oxygen vacancy) and thus modifies its catalytic properties. Here, the catalytic properties of La_2NiO_4 doped with Sr^{2+} and Ca^{2+} toward ORR and OER were investigated in an aqueous alkaline electrolyte, and the catalysts were then incorporated into the cathodes for rechargeable Li–air and Zn–air batteries. We demonstrate for the first time that the doped La_2NiO_4 catalysts exhibit excellent catalytic performance for both ORR and OER, leading to improved round-trip efficiency (reduced voltage gap).

RESULTS AND DISCUSSION

The structural and catalytic properties of A_2MO_4 layered perovskites can be tailored by doping a wide range of aliovalent cations onto the lattice. Taking the ionic radius (r) of La^{3+} (r = 0.1216 nm) into account, in this study, we doped La_2NiO_4 with two different cations that are expected to modify the lattice structure: (i) Sr^{2+} with r = 0.131 nm that is larger than La^{3+} and (ii) Ca^{2+} with r = 0.118 nm that is smaller than La^{3+}.[20] The materials synthesized here are La_2NiO_4 (denoted as LN), $La_{1.9}Ca_{0.1}NiO_4$ (LCN-01), $La_{1.9}Sr_{0.1}NiO_4$ (LSN-01), and $La_{1.7}Sr_{0.3}NiO_4$ (LSN-03). Figure 1b shows the powder X-ray diffraction (XRD) patterns of the undoped and doped La_2NiO_4 catalysts. All of the XRD patterns are consistent with the data for a K_2NiF_4-type layered perovskite structure, which confirms that the partial substitution of Sr^{2+} or Ca^{2+} for La^{3+} does not destroy

dx.doi.org/10.1021/am403244k | ACS Appl. Mater. Interfaces 2013, 5, 9902–9907

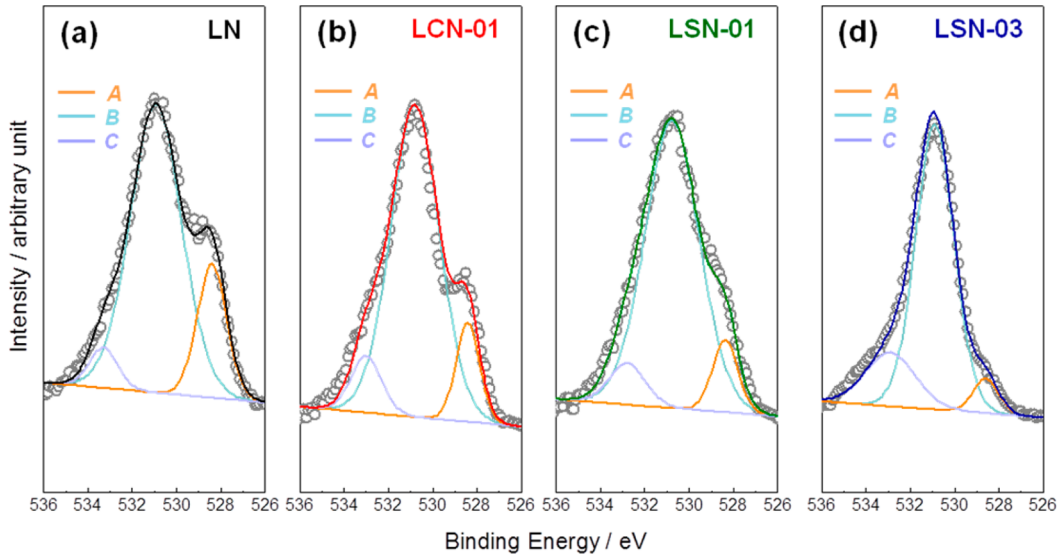

Figure 3. O 1s XPS spectra of (a) La_2NiO_4 (LN), (b) $La_{1.9}Ca_{0.1}NiO_4$ (LCN-01), (c) $La_{1.9}Sr_{0.1}NiO_4$ (LSN-01), and (d) $La_{1.7}Sr_{0.3}NiO_4$ (LSN-03). The symbols and lines represent the measured and fitted spectra, respectively.

the layered characteristics of La_2NiO_4 perovskites, nor does it produce any secondary phases.

To gain detailed information on the crystal structures, the neutron powder diffraction (NPD) patterns of the doped La_2NiO_4 catalysts were collected and analyzed by the Rietveld method. For all of the catalysts, a tetragonal symmetry with *I*4/*mmm* space group was considered in which La, Sr, Ca, and O2 atoms are located at 4*e* (0,0,*z*) sites, Ni at 2*a* (0,0,0), and O1 at 4*c* (0,1/2,0). As shown in Figure 1c−e, the measured NPD data are in good agreement with the calculated results. The refined cell parameters are summarized in Table S1 in the Supporting Information. The following two points should be mentioned regarding the refined results. First, LSN-01 has a larger *c* parameter (1.2714 nm) than LCN-01 (1.2676 nm), which results from the presence of Sr^{2+} larger than Ca^{2+}. A further increase in the *c* parameter was observed for LSN-03. Second, the *a* parameter for LSN-03 is smaller than those of LCN-01 and LSN-01. This indicates an increased oxidation state of Ni in LSN-03, i.e., Ni^{2+} (r = 0.069 nm) → Ni^{3+} (r = 0.060 nm for high spin and r = 0.056 nm for low spin), as a result of charge compensation for Sr^{2+} doping. The TEM study (see Figure S1 in the Supporting Information) indicates that spherical particles as large as 60−100 nm were synthesized by the Pechini method. The lattice fringes with *d*-spacing values of 0.369 and 0.636 nm correspond to the (101) and (002) planes, respectively, which is consistent with the XRD and NPD data. The Brunauer−Emmett−Teller (BET) surface areas of LCN-01, LSN-01, and LSN-03 were determined to be 6.3, 3.7, and 4.3 $m^2\ g^{-1}$, respectively.

The activity of the undoped and doped La_2NiO_4 catalysts for ORR and OER in an aqueous alkaline solution was evaluated by rotating disk electrode (RDE) experiments. Figure 2a presents the polarization (disk current vs potential) curves measured for ORR in 0.1 M KOH. The catalytic activity judged from the onset and half-wave potentials increases in the order of LN < LCN-01 < LSN-01 < LSN-03. This indicates that the cation doping increases the ability to catalyze ORR and that the type and concentration of the dopant play a critical role in the ORR activity. Although the catalysis mechanism is not clearly understood yet, Sr^{2+} (larger than Ca^{2+} and La^{3+}) seems to modify the crystal structure (see the NPD result in Table S1 in the Supporting Information) in such a way as to enhance the activity. According to an atomic simulation study by Read et al.,[18,19] Sr^{2+} was predicted to be more soluble than Ca^{2+} (calculated solution energy = ca. −2.75 eV for Sr^{2+} vs ca. −2.50 eV for Ca^{2+}), suggesting that Ni^{3+} could be more easily formed by Sr^{2+} doping. The TEM results (see Figure S1 in the Supporting Information) show no considerable morphological difference between LCN-01 and LSN-01. Therefore, the higher catalytic activity of LSN-01 might be attributed to the structural and electronic properties modified by cation doping rather than to the morphological difference. Also, higher valence Ni (Ni^{3+}) produced by cation doping is correlated to the activity of nickelate-based catalysts, namely, the activity increases to some extent with an increasing Ni oxidation state.[18,21] This accords with our experimental finding that the ORR activity of Sr^{2+}-doped La_2NiO_4 (LSN-03) with an increased Ni oxidation state is higher than those of LCN-01 and LSN-01. The LSN-03 catalyst exhibits appreciable ORR activity: the onset and half-wave potentials for ORR are ca. 0.91 and 0.83 V vs RHE, respectively.

Another important parameter characterizing the catalyst performance is the number of electrons (n) exchanged during ORR. There are two pathways for ORR in an alkaline electrolyte: (i) reduction of O_2 to OH^- (via four-electron transfer) and (ii) reduction of O_2 to HO_2^- (via two-electron transfer) followed by further reduction of HO_2^- to OH^- or by desorption of HO_2^- into the solution.[22] Thus, the four-electron transfer reaction is a more oxygen-efficient pathway than the two-electron transfer reaction. The n value for the doped La_2NiO_4 catalysts determined from the Koutecky−Levich analysis (see Figure S2 in the Supporting Information) varies between 3.6 and 3.9, whereas n for the catalyst-free KB is about 2.3. This indicates that ORR on the doped La_2NiO_4 catalysts proceeds mainly by the four-electron transfer reaction.

The doped La_2NiO_4 catalysts also display considerable activity toward OER in 0.1 M KOH (Figure 2b). In particular, LSN-03 exhibits higher OER currents over the whole potential range in comparison with LN, LCN-01 and LSN-01. Previous studies of OER kinetics on perovskites[15,23,24] have proposed that the least energetically favorable (rate-determining) step of OER is surface OH^- oxidation and that the oxidation states of transition metals

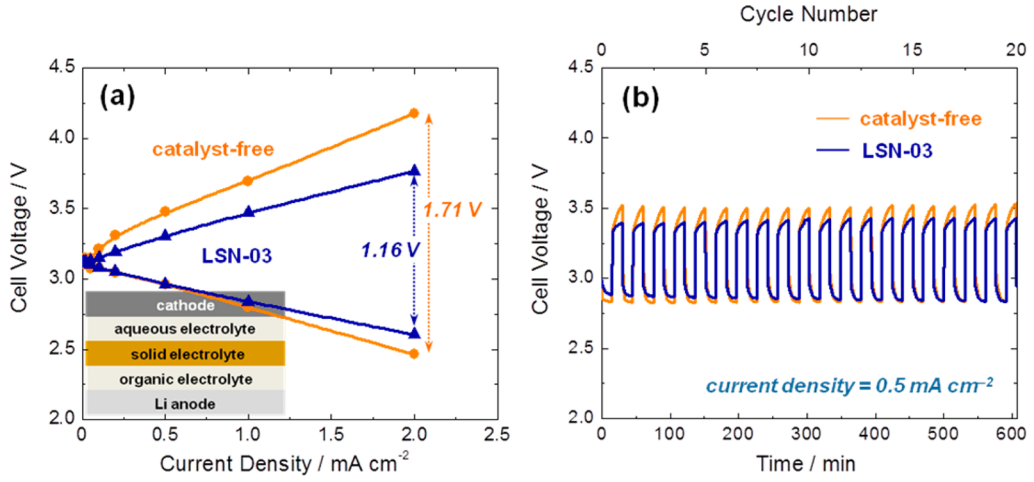

Figure 4. (a) Polarization curves and (b) cycling performance of the hybrid Li-air batteries assembled with the catalyst-free and $La_{1.7}Sr_{0.3}NiO_4$ (LSN-03)-containing cathodes. The Li-air battery consists of a Li metal anode, 1 M $LiPF_6$ in EC/DMC (1:1), an LTAP solid electrolyte, 1 M $LiNO_3$/0.5 M LiOH, and a cathode, as shown in the inset of (a).

and chemical properties of the oxide surfaces (e.g., hydroxide species) have a significant impact on the OER catalysis. The oxygen evolution on nickelate perovskites could be explained in terms of the "Bockris reaction path" in which oxygen atoms in the oxide surface participate directly in OER.[23] Generally, lattice oxygens in nickelate perovskites are loosely bound and hence OER may take place with the direct participation of surface lattice oxygens in the form of OH^- ions. The OER rate is governed by the concentration of hydroxide species that participate in the formation of the O−O bond in hydroperoxide.[15,23−25] In this study, the chemical species present on the undoped and doped La_2NiO_4 surfaces were probed by X-ray photoelectron spectroscopy (XPS), and the measured O 1s spectra are presented in Figure 3. The spectra appear complex, which indicates that more than one type of oxygen species coexist in the surface layer. As shown in Figure 3, the observed spectra were successfully deconvoluted into three component curves (A, B, and C). The low binding energy peak at 528.0−529.8 eV (A) is ascribed to the lattice oxygen in the lanthanum and nickel oxides. Given that rare earth oxides become hygroscopic when exposed to atmospheric conditions, the additional high binding energy peaks at 528.0−533.6 eV (B) and 530.2−535.4 eV (C) originate from hydroxide species and adsorbed water, respectively.[15,26,27]

The relative atomic fractions of the three oxygen species (f_A, f_B, and f_C) were determined from the curves *A*, *B*, and *C*, and then the surface coverage (θ) of hydroxide species was calculated as $\theta = f_B/(f_A + f_B)$. Since the amount of adsorbed water on the as-synthesized sample would depend largely on atmospheric conditions rather than on materials properties, f_C was excluded in the calculation of θ. The θ value was found to increase in the order of LN (0.79) < LCN-01 (0.87) < LSN-01 (0.89) < LSN-03 (0.93), which agrees with the earlier reports suggesting that metals in high oxidation states readily form hydroxide species from water due to an increased ability of the oxide to dissociate water.[14,28] In this work, a clear relationship between the surface coverage of OH^- and the OER activity was observed for the doped La_2NiO_4 catalysts, namely, the higher the surface coverage of hydroxide species, the higher the OER current. Although further investigation is still necessary to explain the composition−activity relationship for layered perovskites, the NPD and XPS results presented here indicate that the enhanced OER activity of LSN-03 may be explained by the higher Ni oxidation state (Figure 1 and Table S1 in the Supporting Information) as well as the larger surface hydroxide coverage (Figure 3).

To prove the efficacy of the doped La_2NiO_4 catalysts in metal-air batteries, the cathode was made using LSN-03, which was identified as the best-performing catalyst in the RDE experiments, and then it was tested in both Li−air and Zn−air batteries under realistic operating conditions. A Li−air battery was constructed with a "hybrid" electrolyte,[29−31] viz., 1 M $LiPF_6$ in EC/DMC (1:1) on the anode side, 1 M $LiNO_3$/0.5 M LiOH on the cathode side, and an $Li_{1+x+y}Ti_{2-x}Al_xSi_yP_{3-y}O_{12}$ (LTAP) solid electrolyte between them. The discharging and charging processes of a hybrid Li−O_2 battery involve ORR and OER in the aqueous electrolyte, respectively. Note that the battery capacity is not governed by cathode activity because the discharge reaction can continue as long as Li^+, O_2, and H_2O are available.[29−31] On the other hand, discharge−charge overpotentials are strongly affected by the ORR-OER kinetics. Therefore, the electrochemical performance of the cathode in a hybrid Li−air battery was judged by the criteria of discharge−charge overpotentials as was done in previously published studies.[29−31]

Figure 4a gives the polarization (cell voltage vs current) curves of the hybrid Li−air batteries assembled with the catalyst-free and LSN-03-containing cathodes. Clearly, the LSN-03 catalyst reduces the overpotentials for discharge and charge over the whole current range. The voltage gap of the battery with LSN-03 is as small as 1.16 V at 2.0 mA cm^{-2}, which is a 550 mV reduction compared to that of the catalyst-free battery. This translates into a 10% increase in the round-trip efficiency, demonstrating that LSN-03 actually functions as an efficient bifunctional catalyst for hybrid Li-air batteries. To provide experimental evidence to support that the layered perovskite structure constributes to the ORR-OER activity, $LaNiO_3$ with a simple perovskite stucture was synthesized and its catalytic properties were studied (see Figures S3−S5 in the Supporting Information). The RDE and battery test results suggest that high activity of the doped La_2NiO_4 catalyst originates from the layered perovskite characteristics as well as the higher Ni oxidation states induced by cation doping.

In addition, the battery constructed with LSN-03 exhibits a stable cycling performance for 20 cycles, as shown in Figure 4b. To understand whether a slight decrease in the discharge voltage

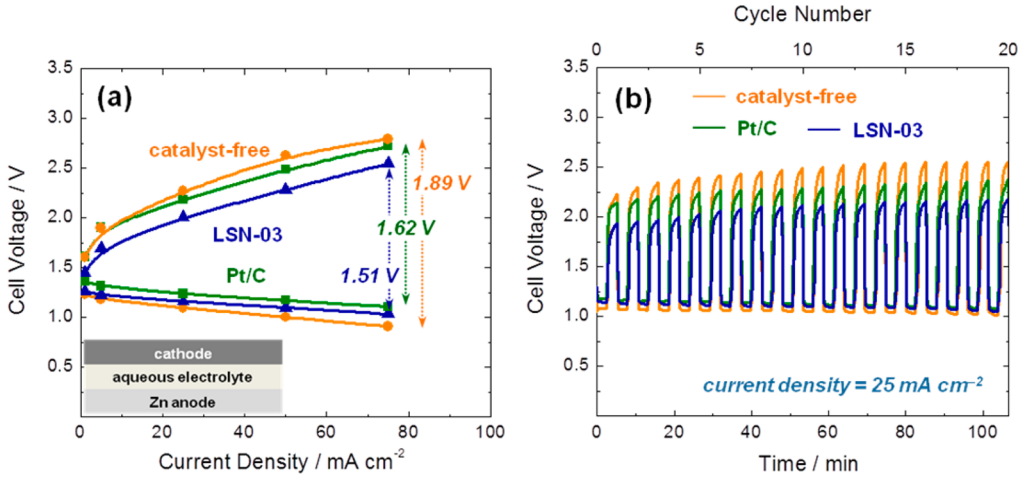

Figure 5. (a) Polarization curves and (b) cycling performance of the Zn-air batteries constructed using the catalyst-free, Pt- and $La_{1.7}Sr_{0.3}NiO_4$ (LSN-03)-containing cathodes. The Zn−air battery is composed of a Zn metal anode, 6 M KOH, and a cathode, as shown in the inset of (a).

is caused by the catalyst degradation, we disassembled the cycled cell and then constructed a new battery using the cycled cathode (i.e., LSN-03-containing cathode taken out of the cycled battery). As shown in Figure S6a in the Supporting Information, the performance was completely recovered, that is to say, the newly assembled battery with the cycled cathode exhibited almost the same initial discharge−charge profile as that of the previous battery with the fresh cathode. Furthermore, Figure S6b in the Supporting Information presents the XRD patterns of the fresh and cycled cathodes, which confirms that the crystal structure of LSN-03 remains stable during cycling. We speculate that other factors are mainly responsible for the observed performance decay, including the growth of lithium dendrites on the anode, the degradation of the LTAP solid membrane, and the oxidation of carbon materials. Further work is currently being conducted to understand the performance degradation during cycling.

The LSN-03 catalyst was also found to significantly reduce the discharge−charge overpotentials of Zn-air batteries (Figure 5a). The electrolyte used was 6 M KOH. When LSN-03 was employed as a cathode catalyst, the voltage gap (~1.51 V) at 75 mA cm^{-2} decreased by 380 mV, leading to an approximately 10% increase in the round-trip efficiency. Remarkably, the voltage gaps for LSN-03 are smaller than those for Pt/C (~1.62 V), which is mainly due to a reduced OER overpotential. Furthermore, high stability was observed for the Zn−air battery assembled with LSN-03, which is in contrast to the noticeable performance degradation of the batteries with the catalyst-free and Pt/C cathodes (Figure 5b).

CONCLUSION

In summary, La_2NiO_4 layered perovskites doped with Sr^{2+} and Ca^{2+} were synthesized and applied as bifunctional catalysts for rechargeable metal-air batteries. The catalysts exhibit high activity toward both oxygen reduction and evolution in an alkaline aqueous solution. The high bifunctional ORR-OER activity leads to remarkably reduced discharge−charge overpotentials (voltage gaps) of Li-air and Zn-air batteries. To the best of our knowledge, this report is the first to demonstrate that cation-doped La_2NiO_4 layered perovskites can serve as efficient bifunctional catalysts for rechargeable metal−air batteries. We expect that increasing the surface area of doped La_2NiO_4 catalysts, for instance, by synthesizing nanocrystals on high-surface area supports, will further improve electrochemical performance.

ASSOCIATED CONTENT

Supporting Information

Experimental details and additional data. This material is available free of charge via the Internet at http://pubs.acs.org.

AUTHOR INFORMATION

Corresponding Author

*E-mail: jjong277@kier.re.kr. Tel.: +82-42-860-3025. Fax.: +82-42-860-3297.

Notes

The authors declare no competing financial interest.

ACKNOWLEDGMENTS

This work was supported by the Energy Efficiency & Resources of KETEP (No. 20112020100110) grant and the Research and Development Program of KIER (B3-2461-08).

REFERENCES

(1) Armand, M.; Tarascon, J. M. *Nature* **2008**, *451*, 652−657.
(2) Neburchilov, V.; Wang, H.; Martin, J. J.; Qu, W. *J. Power Sources* **2010**, *195*, 1271−1291.
(3) Girishkumar, G.; McCloskey, B.; Luntz, A. C.; Swanson, S.; Wilcke, W. *J. Phys. Chem. Lett.* **2010**, *1*, 2193−2203.
(4) Cheng, F.; Chen, J. *Chem. Soc. Rev.* **2012**, *41*, 2172−2192.
(5) Xu, Y.; Ruban, A. V.; Mavrikakis, M. *J. Am. Chem. Soc.* **2004**, *125*, 4717−4725.
(6) Wang, C.; Daimon, H.; Lee, Y.; Kim, J.; Sun, S. *J. Am. Chem. Soc.* **2007**, *129*, 6974−6975.
(7) Lee, Y.; Suntivich, J.; May, K. J.; Perry, E. E.; Shao-Horn, Y. *J. Phys. Chem. Lett.* **2012**, *3*, 399−404.
(8) Prakash, J.; Tryk, D.; Yeager, E. *J. Power Sources* **1990**, *29*, 413−422.
(9) Rios, E.; Gautier, J.-L.; Poillerat, G.; Chartier, P. *Electrochim. Acta* **1998**, *44*, 1491−1497.
(10) Cui, B.; Lin, H.; Li, J.-B.; Li, X.; Yang, J.; Tao, J. *Adv. Funct. Mater.* **2008**, *18*, 1440−1447.
(11) Oh, S. H.; Black, R.; Pomerantseva, E.; Lee, J.-H.; Nazar, L. F. *Nat. Chem* **2012**, *4*, 1004−1010.
(12) Yang, W.; Salim, J.; Li, S.; Sun, C.; Chen, C.; Goodenough, J. B.; Kim, Y. *J. Mater. Chem.* **2012**, *22*, 18902−18907.
(13) Jung, K.-N.; Lee, J.-I.; Yoon, S.; Yeon, S.-H.; Chang, W.; Shin, K.-H.; Lee, J.-W. *J. Mater. Chem.* **2012**, *22*, 21845−21848.

(14) Malkhandi, S.; Yang, B.; Manohar, A. K.; Manivannan, A.; Surya, Prakash, G. K.; Narayanan, S. R. *J. Phys. Chem. Lett.* **2012**, *3*, 967−972.
(15) Hardin, W. G.; Slanac, D. A.; Wang, X.; Dai, S.; Johnston, K. P.; Stevenson, K. J. *J. Phys. Chem. Lett.* **2013**, *4*, 1254−1259.
(16) Jin, C.; Cao, X.; Zhang, L.; Zhang, C.; Yang, R. *J. Power Sources* **2013**, *241*, 225−230.
(17) Takeguchi, T.; Yamanaka, T.; Takahashi, H.; Watanabe, H.; Kuroki, T.; Nakanishi, H.; Orikasa, Y.; Uchimoto, Y.; Takano, H.; Ohguri, N.; Matsuda, M.; Murota, T.; Uosaki, K.; Ueda, W. *J. Am. Chem. Soc.* **2013**, *135*, 11125−11130.
(18) Read, M. S. D.; Islam, M. S.; King, F.; Hancock, F. E. *J. Phys. Chem. B* **1999**, *103*, 1558−1562.
(19) Read, M. S. D.; Islam, M. S.; Watson, G. W.; Hancock, F. E. *J. Mater. Chem.* **2001**, *11*, 2597−2602.
(20) Shen, Y.; Zhao, H.; Świerczek, K.; Du, Z.; Xie, Z. *J. Power Sources* **2013**, *240*, 759−765.
(21) King, F.; Hancock, F. E. *Catal. Today* **1996**, *27*, 203.
(22) Cheng, F.; Su, Y.; Liang, J.; Tao, Z.; Chen. *J. Chem. Mater.* **2010**, *22*, 898−905.
(23) Bockris, J. O.; Otagawa, T. *J. Phys. Chem.* **1983**, *87*, 2960−2971.
(24) Suntivich, J.; May, K. J.; Gasteiger, H. A.; Goodenough, J. B.; Shao-Horn, Y. *Science* **2011**, *334*, 1383−1385.
(25) Rossmeisl, J.; Qu, Z. W.; Zhu, H.; Kroes, G. J.; Norskov, J. K. *J. Electroanal. Chem.* **2007**, *607*, 83−89.
(26) Choisnet, J.; Abadzhieva, N.; Stefanov, P.; Klissurski, D.; Bassat, J. M.; Rives, V.; Minchev, L. *J. Chem. Soc. ,Faraday Trans.* **1994**, *90*, 1987−1991.
(27) Ma, Z.; Gao, X.; Yuan, X.; Zhang, L.; Zhu, Y.; Li, Z. *Catal. Commun.* **2011**, *12*, 817−821.
(28) Wu, N.-L.; Liu, W.-R.; Su, S.-J. *Electrochim. Acta* **2003**, *48*, 1567−1571.
(29) Wang, Y.; Zhou, H. *J. Power Sources* **2010**, *195*, 358−361.
(30) Yoo, E.; Zhou, H. *ACS Nano* **2011**, *5*, 3020−3026.
(31) He, H.; Niu, W.; Asl, N. M.; Salim, J.; Chen, R.; Kim, Y. *Electrochim. Acta* **2012**, *67*, 87−94.